

Space efficient implementation of hypergraph dualization in the D -basis algorithm

Skylar Homan¹, Anoop Krishnadas², and Kira Adaricheva^{*3}

¹Programs Department, AMS

²School of Engineering, Hofstra University

³Department of Mathematics, Hofstra University

Abstract

We present a new implementation of the D -basis algorithm called the *Small Space* which considerably reduces the algorithm's memory usage for data analysis applications. The previous implementation delivers the complete set of implications that hold on the set of attributes of an input binary table. In the new version, the only output is the frequencies of attributes that appear in the antecedents of implications from the D -basis, with a fixed consequent attribute. Such frequencies, rather than the implications themselves, became the primary focus in analysis of datasets where the D -basis has been applied over the last decade. The D -basis employs a hypergraph dualization algorithm, and a dualization implementation known as *Reverse Search* allows for the gradual computation of frequencies without the need for storing all discovered implications. We demonstrate the effectiveness of the Small Space implementation by comparing the runtimes and maximum memory usage of this new version with the current implementation.

Keywords: Implications, binary table, the D -basis algorithm, hypergraph dualization

1 Introduction

In data mining, the retrieval and sorting of association rules is a research problem of considerable interest. Association rules uncover the relationships between the attributes of a set of objects recorded in a binary table.

This, for example, can be a medical data table, where the objects/rows are patients and the attributes/columns are indicators of some property, such as a genetic marker or record of a particular treatment, that may or may not hold in a patient: position (r, c) in the table, in row r and column c , is 1 if property c occurs in patient r ; otherwise, it is 0.

The algorithm known as *Apriori* remains a common tool for extraction of association rules from binary data and was included in libraries of R and Microsoft office. One of the more recent surveys on association rules is in [9].

One particular subset of association rules known as *implications*, or rules of full confidence, merit particular attention in data mining, as well as being at the center of ongoing theoretical study ([12, 26]). From a practical point of view, implications are the strongest rules available on a given table because they hold true for any row of the table.

The retrieval of a set of implications as an equivalent representation of a binary table has been developed using ideas from Formal Concept Analysis (FCA); see [18]. It is based on the fact that the table generates a unique closure operator on the set of its attributes, and thus can be associated with the lattice of the closed set of this operator, also known as the *Galois lattice* or *the concept lattice*. The standard approach in FCA is to build the concept lattice, then retrieve its set of implications, known as the *canonical basis*. The size of the concept lattice is exponential on the size of the table,

*Corresponding author; email: Kira.Adaricheva@hofstra.edu

and the retrieval of the canonical basis is co-NP complete [8]; thus, these algorithms are practical only for tables of small size.

A new approach was taken in [3], where the canonical basis of the concept lattice is replaced by the D -basis, a set of implications with a background in the study of free lattices [17]. The key difference compared to the canonical basis approach is that the computation of the D -basis does not require the whole concept lattice. Instead, the D -relation on the reduced set of attributes is used to find a portion of the D -basis associated with a particular consequent t from the set of attributes. The crucial advantage is in the use of a *hypergraph dualization* algorithm on the specific hypergraph associated with the attribute t and the D -relation. The edges of the dual hypergraph are used to produce the output of the D -basis implications. This algorithm was dubbed the *D -basis algorithm*.

Since the D -basis approach employs hypergraph dualization, which is an algorithm with sub-exponential time complexity based on the size of the input and output, the D -basis is very effective in terms of the time spent to generate any given implication in the output. On the other hand, it contains considerably more implications than the canonical basis, and thus may require a larger amount of space for its output. The output shows this exponential tendency, per testing results done on a series of tables of increasing size with the density of ones in the middle range of 0.3-0.7 [24].

In the current project, a new approach was taken with respect to the usage of hypergraph dualization in the implementation of the D -basis algorithm.

Observe that in many applications, only the aggregate values related to frequencies of attributes that appear in implications were needed, as opposed to requiring the complete list of implications; see [5, 6, 22]. These aggregate values can be updated every time a transversal is found during the hypergraph dualization stage of the algorithm. This task can be achieved using the *Reverse Search* implementation of dualization described in [21].

The new implementation of the D -basis algorithm, called the *Small Space*, makes use of the enumerative properties of Reverse Search to relocate the aggregate computation into the hypergraph dualization stage of the algorithm without affecting its output accuracy. This removes the need to allocate space for recording and transferring the list of implications between the stages of the algorithm.

In section 2, we introduce important concepts to provide for the background of the D -basis algorithm as it is formulated in Theorem 1 [3]. Section 3 gives an overview of the attribute ranking process of tabled data with respect to a set of implications, which was developed as part of the D -basis output in [7]. In particular, we demonstrate the key difference between the existing version and the new *Small Space* version of the D -basis algorithm. In Section 4, we provide test results of the Small Space algorithm side by side with the existing D -basis algorithm that demonstrate the space savings when the new version of the algorithm is used.

2 Tables, closure systems, implicational bases and hypergraphs

In this section we will follow a simple example to present the major concepts and the mathematical background of the D -basis algorithm. Many additional details can be found in [3].

We will call $T = (U, A, R)$ a binary table if A, U are finite sets and $R \subseteq U \times A$ a *relation* between U and A . U is called a set of objects and A a set of attributes.

Example 1. Let $T = (U, A, R)$ be a binary table given in Table 1. Here $U = \{1, 2, \dots, 9\}$, $A = \{t, a_1, a_2, b_1, b_2, c\}$ and pairs from R are marked by 1 in the table.

For any subset $Y \subseteq A$ there exists $Z \subseteq U$ such that $z \in Z$ iff $(z, y) \in R$ for all $y \in Y$. Z is called a *support* of Y and denoted $Z = \text{sup}(Y)$. This formally defines mapping $\text{sup}_A : 2^A \rightarrow 2^U$, a support function on A . Symmetrically, sup_U can be defined on U .

Example 2. In Table 1, $\text{sup}_A(\{a_2, b_2\}) = \{3, 5, 8, 9\}$ and $\text{sup}_U(\{6, 7\}) = \{b_1, b_2\}$.

It is a standard and easy argument to show that $\phi_A : 2^A \rightarrow 2^A$, defined as $\phi_A(Y) = \text{sup}_U(\text{sup}_A(Y))$ for any $Y \in 2^A$, is a *closure operator*, i.e., it is increasing, monotone and idempotent. Sets $\phi_A(Y)$, $Y \in 2^A$, form a *closure system*, i.e., a set system with a family of subsets of A closed under intersection and containing A itself. Such a family always forms a lattice with respect to the inclusion order. This

Table 1: Binary table with 6 attributes

$U \setminus A$	t	a_1	a_2	b_1	b_2	s
1	0	1	0	1	0	0
2	1	0	0	1	1	0
3	0	0	1	0	1	1
4	0	0	0	1	1	0
5	1	1	1	1	1	0
6	0	0	0	1	1	0
7	1	0	0	1	1	0
8	1	1	1	1	1	1
9	1	1	1	1	1	0

lattice $L(T)$ is called the *Galois lattice*, or the *concept lattice* of table $T = (U, A, R)$. We mention that the table is called *reduced* when operator ϕ_A is *standard*, i.e. satisfies the condition that $\phi_A(\{y\}) \setminus \{y\}$ is closed for every $y \in A$. In such a case, set A is in one-to-one correspondence with the set of join irreducible elements of lattice $L(T)$, which are exactly $\phi_A(y)$, $y \in A$.

Note that one can symmetrically define the closure operator $\phi^* : 2^U \rightarrow 2^U$ on the set U by setting $\phi^*(Z) = \sup_A(\sup_U(Z))$ for any $Z \in 2^U$. The resulting lattice of closed sets is $L^*(T)$, which is dual to $L(T)$. One can follow monographs [13, 10, 18] on the topic.

Example 3. One can check that $\phi(\{t\}) = \{t, b_1, b_2\}$ and $\phi^*(\{8, 9\}) = \{5, 8, 9\}$. The Hasse diagram of $L(T)$ is on Figure 1, where x marks set $\phi(\{x\})$ for all $x \in A = \{a_1, a_2, b_1, b_2, s, t\}$.

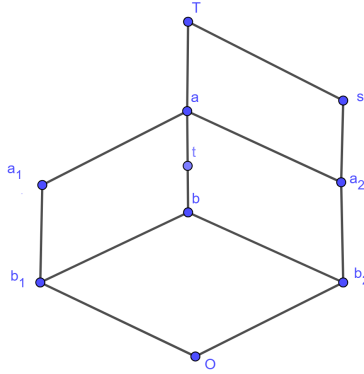


Figure 1: The Galois lattice $L(T)$ of Table 1

It is typical to retain partial information about a closure operator ϕ on set A known as an *implicational basis* (IB) so that the operator can be fully recovered from it. Every IB can be represented as a set of pairs $(X, Y) \subseteq 2^A \times 2^A$ such that $Y \subseteq \phi(X)$; more often, such pairs are written as an implication $X \rightarrow Y$.

Example 4. It was established in the previous Example that $\phi(\{t\}) = \{t, b_1, b_2\}$, which can be written as the implication $t \rightarrow b_1 b_2$. Its meaning in Table T is that in every row of the table where the entry for column t is marked by 1, the entries for columns b_1 and b_2 in that row are also marked by 1.

For any IB there is a unique corresponding closure operator, but there are multiple IBs for the same closure operator.

A well known example of an IB is the *canonical* basis, or Guigues-Duquenne basis ([19]), $\Sigma_c = \{P \rightarrow \phi(P) : P \subseteq A \text{ is a pseudo-closed set}\}$. The canonical basis is known for having the minimal number of implications defining the closure operator. See [25] for details.

Before proceeding to the description of another IB known as the *D-basis*, it is necessary to introduce the concepts of a hypergraph and its dual.

A *hypergraph* is a pair of a set and a family of subsets: $\mathcal{H} = \langle A, \mathcal{F} \rangle$, $\mathcal{F} \subseteq 2^A$. A *transversal* of the hypergraph is $Y \subseteq A$ such that $Y \cap F \neq \emptyset$ for every $F \in \mathcal{F}$. Y is called *minimal* if $Y \setminus y$ is not a transversal for every $y \in Y$. The hypergraph $\mathcal{H}^d = \langle A, \mathcal{T} \rangle$, where \mathcal{T} is a set of minimal transversals of $\mathcal{H} = \langle A, \mathcal{F} \rangle$, is called the *dual* of \mathcal{H} .

The problem of finding \mathcal{H}^d for a given hypergraph $\mathcal{H} = \langle A, \mathcal{F} \rangle$ is called *dualization*. Dualization is an enumeration algorithm, i.e. one that produces all required objects and does so without repetitions. In the case of dualizing a hypergraph \mathcal{H} , all minimal transversals of \mathcal{H} have to be produced, and each must appear in the output only once. Many optimization problems reduce to the task of dualization of some hypergraph, which makes this problem very important in applied mathematics and computer science.

It turns out that the dualization of the hypergraph can be incorporated into the procedure of finding the *D-basis*.

The *D-basis* was introduced in [2] and belongs to the family of *unit* bases, i.e. IBs comprised of implications $Y \rightarrow x$, with $Y \subseteq A$ and $x \in A$. While there is no technical difference between unit bases and arbitrary IBs, the focus of the unit implication is on the consequent element x rather than the set Y in the left side of implication. In particular, the *D-basis* was defined as the implicational equivalent of the *join cover relations* known in lattice theory as the way to define lattices.

More precisely, every element of a finite lattice L is a join of join irreducible elements, the set of which is denoted $\text{Ji}(L)$, so the relation can be written in the form $x \leq \bigvee Y$, for $x \in \text{Ji}(L)$ and $Y \subseteq \text{Ji}(L)$. If $Y = \{y\}$, then this is the order relation $x \leq y$ for some elements $x, y \in \text{Ji}(L)$, and these relations are included in any IB. Otherwise, Y is called a *non-trivial minimal join cover* for x if $x \not\leq y$ for $y \in Y$ and none of $y \in Y$ can be replaced by smaller elements in L and still produce a cover for x .

Example 5. $t \leq a_1 \vee s$ is a non-trivial join cover for t in lattice $L(T)$ on Figure 1, but it is not a minimal cover, because $t \leq a_1 \vee b_2$, for $b_2 < s$, and neither a_1 nor b_2 can be replaced by smaller elements to make a join cover for t .

Every lattice L with $A = \text{Ji}(L)$ can be represented as a closure system on set A with the closure operator ϕ defined by the IB comprising *binary implications* $y \rightarrow x$ for all relations $x \leq y$, and $Y \rightarrow x$ for minimal covers $x \leq \bigvee Y$ in L . This IB is called the *D-basis* [2].

Example 6. The *D-basis* for $L(T)$ on Figure 1 consists of binary implications $a_1 \rightarrow b_1$, $t \rightarrow b_1$, $t \rightarrow b_2$, $a_2 \rightarrow b_2$, $s \rightarrow a_2$, and $s \rightarrow b_2$; and non-binary implications $a_1 b_2 \rightarrow t$, $a_1 b_2 \rightarrow a_2$, $b_1 a_2 \rightarrow t$ and $b_1 a_2 \rightarrow a_1$.

The *D-relation* on $\text{Ji}(L)$ can be defined independently of the *D-basis*, but the following is a necessary and sufficient condition ([17]):

$x D y$ iff $y \in Y$ for some non-binary implication $Y \rightarrow x$ in the *D-basis*.

Now we connect this with the *D-relation* as it is identified in a table T with Galois lattice $L(T)$.

There exist additional relations $\uparrow, \downarrow, \downarrow\downarrow$ between sets U, A that can be easily computed given $T = (U, A, R)$. Many properties of the Galois lattice can be expressed in the language of these relations [18]. It is the case that $\uparrow, \downarrow, \downarrow\downarrow \subseteq (U \times A) \setminus R$, and the *D-relation* on set A can be computed using \uparrow, \downarrow ([17]):

For any $x, y \in A$, $x D y$ iff there exists $u \in U$ such that $(u, x) \in \uparrow$ and $(u, y) \in \downarrow$.

Further details can be found in [3]. We denote $x D = \{y \in A : x D y\}$.

Example 7. In Table 1, $(3, t) \in \uparrow$ and $(3, b_1) \in \downarrow$, therefore, $t D b_1$. In fact, $t D = \{a_1, a_2, b_1, b_2\}$.

Now we want to explore the possibility of finding the D -covers for one of elements in A . For example, given binary table $T = (U, A, R)$, suppose that one needs to find all possible implications $Y \rightarrow x$ for a fixed element $x \in A$ and some $Y \subseteq A$. In such a setting, element $x \in A$ is called a *target*. It is easy to find trivial covers for x directly in the table, so we focus on non-trivial ones.

This is a task suitable for a unit basis such as the D -basis, because it is equivalent to the task of finding all non-trivial minimal join covers $x \leq \bigvee Y$ in lattice $L(T)$ for that element x . (Recall that $x \in A$ corresponds to $\phi(x) \in L(T)$, so we can continue calling $\phi(x)$ as x .)

Note that since $x \leq \bigvee Y$, then $\bigvee Y$ is one of the elements in interval $[x, 1_L] \subseteq L(T)$, while we need to pick elements for Y in $L(T) \setminus [x, 1_L]$.

Denote $M(x) = \{M_1, \dots, M_k\}$ as the set of maximal elements in the poset $L(T) \setminus [x, 1_L]$. Then $\bigvee Y \not\leq M_i$, so $Y \not\subseteq M_i$ for all $i \leq k$. Therefore, Y should have a non-empty intersection with $A \setminus M_i$ for each $i \leq k$. Additionally, we want Y to be a non-trivial minimal cover, i.e. $Y \subseteq xD$. Therefore, Y should have a non-empty intersection with all sets $xD \setminus M_1, \dots, xD \setminus M_k$. Moreover, due to the definition of a minimal cover, $|Y|$ is minimal with this property.

This makes Y a *minimal transversal* in hypergraph $\mathcal{H}(x) = \langle xD, \{xD \setminus M_1, \dots, xD \setminus M_k\} \rangle$.

The argument above is an outline of the following result in [3].

Theorem 1. *Given (reduced) table $T = (U, A, R)$, consider closure operator ϕ_A , $x \in A$ and related hypergraph $\mathcal{H}(x) = \langle xD, \{xD \setminus M_1, \dots, xD \setminus M_k\} \rangle$. Then for any non-binary implication $Y \rightarrow x$ in the D -basis of operator ϕ_A , set Y is a minimal transversal of $\mathcal{H}(x)$.*

Example 8. Consider the target $t \in A$, for Table 1. Removing $[t, 1_L]$ from $L(T)$ in Figure 1, we get a poset with three maximal elements: a_1 , s and $b_1 \vee b_2$. Seeing the same lattice as a closure lattice of operator ϕ , these are closed sets $M_1 = \{a_1, b_1\}$, $M_2 = \{s, a_2, b_2\}$ and $M_3 = \{b_1, b_2\}$. These elements can be easily found directly in the table: they correspond to $u \in U$ such that $(u, x) \in \uparrow$; in the case of Table 1: $u = 1, 3, 4$ and $M_1 = \sup_U(1)$, $M_2 = \sup_U(3)$, $M_3 = \sup_U(4)$. Then the related hypergraph $\mathcal{H}(t) = \langle tD, \{tD \setminus M_1, \dots, tD \setminus M_3\} \rangle = \langle \{a_1, a_2, b_1, b_2\}, \{a_1b_1, a_2b_2, a_1a_2\} \rangle$.

It is easy to find the minimal transversals: a_1b_2, a_2b_1, a_1a_2 . As Theorem 1 claims, the left sides of both D -basis implications $a_1b_2 \rightarrow t, a_2b_1 \rightarrow t$ are present among minimal transversals.

Note that Theorem 1 only states that every implication $Y \rightarrow x$ from the D -basis will be accounted for among the minimal transversals of a specific hypergraph $\mathcal{H}(x)$. On the other hand, there might be transversals that do not represent an implication from the D -basis, but they necessarily represent implications from a larger basis known as the *canonical direct unit basis*; see [11]. The paper [4] provides a new version of the algorithm for the exact retrieval of the D -basis based on the dualization in distributive lattices [15]. It could support a new code implementation of the D -basis in the future.

For both the Small Space and the current implementation of the D -basis, the time complexity is defined by the time complexity of the hypergraph dualization stage. In the seminal paper [16] the time complexity of the algorithm for the dualization of a hypergraph was shown to have a sub-exponential upper bound based on the combined size of the input and output. The question of whether there exists such an algorithm with polynomial time complexity remains open. Multiple algorithms for dualization are presented and analyzed in [21].

In particular, the Reverse Search (RS) algorithm relies on the concept of a critical hyperedge to guide the search for minimal transversals without needing to check its output against a list of transversals already found, which makes the search effective in both time and space while still finding every minimal transversal only once.

These characteristics make the RS algorithm ideal when moving the “update frequencies” functionality into the hypergraph dualization process, as hyperedges can be discarded rather than stored without affecting the enumeration behavior of the RS algorithm. The next section gives more details on the essence of this change and its importance for reducing memory usage in data analysis applications.

3 Ranking attributes relevant to a target attribute

In this section we outline the “accounting” function that the current D -basis implementation performs. We note that this particular function does not need to deal with implications of the D -basis, and

instead can be applied to any set \mathcal{T} of association rules or implications. When such a set \mathcal{T} is available, one can measure the frequency of any attribute y appearing in the antecedents of the rules $Y \rightarrow t$ in \mathcal{T} , together with other attributes. One advantage of such an approach is that the typically high volume of rules found in the table provides a good representation of all attributes and allows for better comparison of attributes related to a given target.

For the purposes of the D -basis algorithm, \mathcal{T} is one of two sets. One is $\mathcal{T}(t, \delta)$, the set of implications $Y \rightarrow t$ in the D -basis, with some fixed target $t \in A$ and value $\delta > 0$ so that $|\sup_A(Y \cup t)| \geq \delta$. Here δ is the *minimal support*, which says that, for every implication in $\mathcal{T}(t, \delta)$, there exist at least δ rows of table $T = (U, A, R)$ that support it. The second set $\mathcal{T}(\neg t, \delta)$ is similar, except t is replaced by $\neg t$, which may or may not be a member of A . When $\neg t$ is not in the table, one needs to modify the table by adding $\neg t$ (or replacing t with $\neg t$) before running the algorithm.

Let us give a more precise definition of how the relevance of attribute y with respect to target attribute t is computed. For each attribute $y \in A \setminus t$ and some $\delta > 0$, the *relevance* of y to $t \in A$ is a ratio of two parameters of *total support*. One is computed with respect to set $\mathcal{T}(t, \delta)$ of implications describing the table:

$$\text{tsup}_t(y) = \Sigma \left\{ \frac{|\sup_A(Y)|}{|Y|} : y \in Y, (Y \rightarrow t) \in \mathcal{T}(t, \delta) \right\}. \quad (1)$$

Thus $\text{tsup}_t(y)$ shows the frequency of attribute y appearing together with some other attributes in implications $Y \rightarrow t$ of the basis $\mathcal{T}(t, \delta)$. The contribution of each implication $Y \rightarrow y$, where $y \in Y$, to the total support computed for y is higher when $\sup_A(Y)$ is higher, but also when the antecedent Y has fewer other attributes besides y .

Example 9. The following data set has been converted to a binary form from a snippet of real data from 10 patients with two types of liver cancer. This data was tested during the initial implementation of the D -basis algorithm leading to publication [7].

```

1 0 0 0 0 1 0 0 0 1 1 0 1 1 0 1 1 1 0 1 1 1
1 1 1 0 0 1 0 0 1 1 1 0 0 0 1 1 0 1 0 1 0 1
1 1 1 1 0 1 1 1 1 1 1 1 1 0 0 0 0 0 0 0 0 1
1 1 0 1 0 1 1 1 0 0 0 0 1 1 1 0 0 0 1 1 1 1
0 0 1 1 1 1 1 1 1 1 1 1 1 1 1 1 1 1 1 0 0 0
0 0 0 1 1 1 1 1 0 0 1 1 0 0 1 1 0 0 0 1 1 0
1 1 1 1 1 1 1 1 0 1 0 1 0 1 0 1 0 1 0 1 0 1
1 1 0 1 0 1 1 1 1 1 0 1 1 1 1 1 1 1 0 1 1 1
1 1 0 0 0 1 1 1 0 0 0 0 0 0 0 1 1 1 1 0 0 0
0 0 0 0 1 1 1 1 0 0 0 0 1 1 1 1 0 0 0 0 1 1

```

The set of implications $\mathcal{T}(22, 3)$ was requested with the target attribute $t = 22$, which is the last column in the table, and $\text{minsup} = 3$. The algorithm produced 17 implications with the consequent $t = 22$ and support ranging between 3 and 6. The output includes information about reduced columns and lists all implications with their supports and the list of rows where each implication is validated:

6 \Leftrightarrow Note: column 6 is reduced, a column with all 1s
8 \Leftrightarrow 7 Note: column 8 is reduced, equal to column 7

1; 1 4 \rightarrow 22 ; Support = 4; rows = 3, 4, 7, 8,

2; 1 10 \rightarrow 22 ; Support = 5; rows = 1, 2, 3, 7, 8,

3; 1 11 \rightarrow 22 ; Support = 4; rows = 1, 2, 3, 8,

4; 1 21 \rightarrow 22 ; Support = 3; rows = 1, 4, 8,

...

17; 21 14 \rightarrow 22 ; Support = 4; rows = 1, 4, 8, 10

The last part of the output provides the total supports for all attributes that participate in produced set of implications $\mathcal{T}(22, 3)$, computed according to equation (1):

Column y	1	...	4	...	10	11	12	13	14	15	...	18	19	20	21	22
$tsup_{22}(y)$	10.67	0	2	0	3	2	0	3.67	4	1	0	1.33	0	6.67	3.67	0

For example, attribute 4 appears only in implication #1, and its contribution to the total support is given by:

$$\frac{Support(1\ 4 \rightarrow 22)}{|\{1, 4\}|} = 2.$$

While the frequent appearance of a particular attribute y in implications $Y \rightarrow t$ might indicate the relevance of y to t , the same attribute may appear in implications $U \rightarrow \neg t$.

Let $\mathcal{T}(\neg t, \delta)$ be the basis of closure system obtained after replacing the original column of attribute t by its complement column $\neg t$. Then the *total support* of $\neg t$ can be computed, for each $y \in A \setminus t$, as before:

$$tsup_{\neg t}(y) = \Sigma \left\{ \frac{|sup(U)|}{|U|} : y \in U, (U \rightarrow \neg t) \in \mathcal{T}(\neg t, \delta) \right\}.$$

Now define the parameter of *relevance* of attribute $y \in A \setminus t$ to attribute t , with respect to the pair of bases $\mathcal{T}(t, \delta)$ and $\mathcal{T}(\neg t, \delta)$:

$$rel_t(a) = \frac{tsup_t(y)}{tsup_{\neg t}(y) + 1}. \quad (2)$$

A high relevance of y to t is achieved by a combination of high total support of y for implications $Y \rightarrow t$ and low total support for implications $U \rightarrow \neg t$. This parameter provides a ranking of all attributes $y \in A \setminus t$.

Note that the ranking of all attributes in relation to a particular target attribute was introduced in [7], together with the first application of the *D*-basis algorithm in data analysis. It was later successfully applied for analysis of survival probability in patients with stomach cancer in [22], when the number of attributes (gene expressions) was reduced to about 500 by other methods. There was no direct analysis of the implications found, due to the sheer size of the output sets.

This aspect of implications and, more generally, association rules found in attributes of binary data is discussed in [20, 9], with the goal of restricting the attention to concise subsets of rules that would also allow some logical inference.

Instead, the approach with the ranking proposed in [7] relies on a statistical treatment of rules, where a particular statistic called the *relevance* given by equation (2) indicates that a particular attribute may have a higher or lower probability of appearing in implications with the given target.

From the point of computational effectiveness, this approach allows the algorithm to keep less information in the output: the total support values for each attribute can be returned alone, rather than the whole set of implications.

3.1 Small Space version of the *D*-basis algorithm

In this section we describe the flow of the current version of the *D*-basis algorithm, then demonstrate the modifications made to this flow in the Small Space version.

The code and documentation of the *D*-basis algorithm is available through the public Git repository <https://gitlab.com/npar/dbasis>.

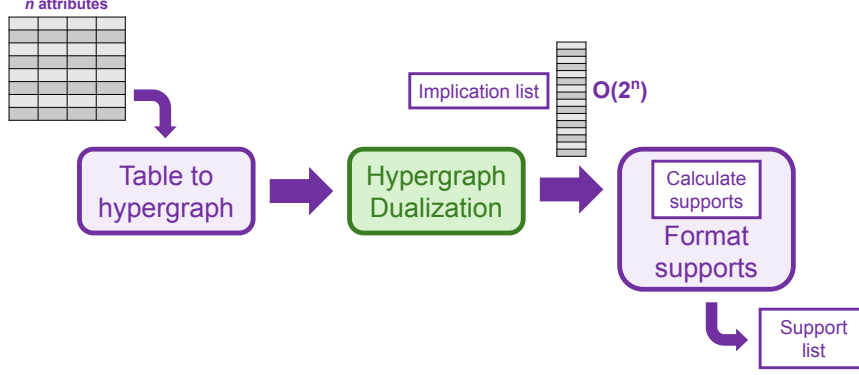


Figure 2: Flow of the D -basis algorithm

Referring to Fig.2, here are the main phases of the algorithm:

1. The algorithm is initialized with the binary table, together with several parameters: the index of the target column t , the minimum support $minsup$ of implications accepted for the output, and the name of the specific implementation of hypergraph dualization (HD) to be used by the algorithm.
2. The table is reduced, the D -relation for t is computed, and the hypergraph $\mathcal{H}(t)$ is passed to the specified HD library.
3. The HD library produces the dual hypergraph $\mathcal{H}^d(t)$, whose hyperedges are passed back to the main unit.
4. Hyperedges returned by HD are used to form implications with t as a consequent and checked against the original table to ensure they pass the $minsup$ threshold. Implications which do not have a support of at least $minsup$ are discarded.
5. For every implication $Y \rightarrow t$ which meets the $minsup$ requirement, its contribution to the total support of each attribute appearing in Y is calculated, and an array of total supports is updated with these contributions.
6. The output includes the list of all implications and the total supports array.

Fig. 3 shows the flow of the modified version of the algorithm, called the Small Space D -basis.

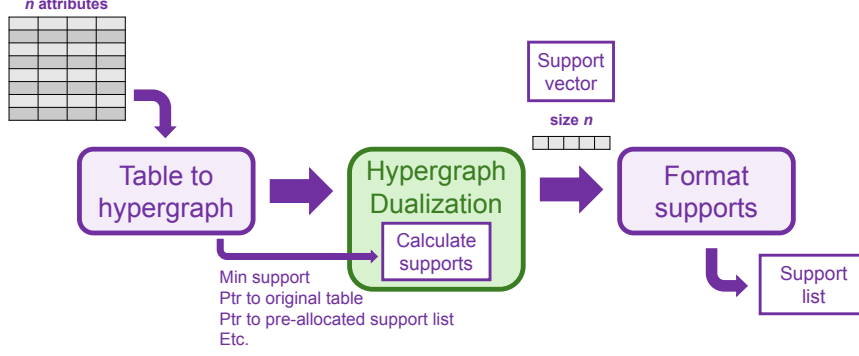


Figure 3: Small Space D -basis algorithm

- The algorithm starts similarly, being initialized with the binary table, the index of the target column t , and the minimum support $minsup$ of implications for the output. The choice of HD algorithm is restricted to RS (Reverse Search).
- The table is reduced, and the D -relation for t is computed. The hypergraph $\mathcal{H}(t)$ is passed to the RS algorithm in the HD library, along with pointers to original representation of the binary table and an empty array allocated for total supports.
- The RS algorithm generates the dual hypergraph $\mathcal{H}^d(t)$ one transversal at a time. When a minimal transversal Y is found, the implication $Y \rightarrow t$ is immediately tested on the original table to ensure it passes the $minsup$ threshold. If the $minsup$ threshold is passed, its contribution to the total support of each attribute in Y is calculated, and the total supports array is updated. The hyperedge Y is then discarded, rather than being stored.
- After the RS algorithm has run, the total supports array is passed back to the main unit. As hyperedges were not stored in the previous step, no list of implications is returned by the HD library.
- The output includes only the total supports array.

By calculating the total support contribution of each edge as it is found during HD, the Small Space algorithm bypasses the need to store the entire list of hyperedges in $\mathcal{H}^d(t)$ at once. As this list has size complexity $O(2^n)$ relative to the number of attributes in the input table, it is easily the fastest-growing source of memory consumption in the D -basis algorithm. Therefore, in data analysis applications on large datasets ([5], [6], [22]), where only the total supports are required to identify relevant attributes, eliminating the need to store the implication list can dramatically reduce the algorithm’s maximum memory usage on larger datasets.

4 Testing results

Here we present the results of the Small Space testing for several data sets. The open-source program Valgrind (<https://valgrind.org/>) was used to track memory usage, instruction count, and program runtime over the duration of the algorithm’s run. Specifically, we used the Massif tool, which is a heap profiler provided by Valgrind to track the memory use over total memory use, time, and instruction use as separate tests.

Tests were performed in a Docker container, hosted on a laptop computer with an AMD Ryzen 7 5800H processor. For each column t of the table, Valgrind was used to run the original D -basis

algorithm with target t three times, measuring the maximum memory utilization of the first run, the number of instructions executed during the second run, and the runtime (in milliseconds) of the third run. All test runs used a minimum support of 1, so vacuously true implications were excluded, but all implications supported by at least one row of the input table were permitted. This same process was then repeated using the Small Space algorithm. Results were recorded for all six runs and compared against one another to evaluate the impact of the Small Space’s changes.

Because the speed at which an algorithm is executed is dependent on the specifications of the system executing it, the number of processor instructions executed during a run of the program, as well as the actual runtime in milliseconds, are used to evaluate the speed and complexity of the algorithm. As the speed of execution can vary based on how many other tasks a program is sharing the processor with, runtime is a less reliable measurement, as it may be prone to fluctuation due to uncontrolled outside factors. Testing attempted to mitigate this by keeping as few other tasks running as possible, but runtime results should still be considered rough estimates rather than precise measurements.

The data sets and instructions on how to use the D -basis code and read the output are given in the repository: https://gitlab.com/npar/dbasis/-/tree/pipeline_testing

4.1 STEM dataset

The first testing dataset was taken from the data involved in publication [5], where the first and third authors were involved in as co-authors. This data comprises the records of about 100 undergraduate students in academic years 2010-2015, who majored in Biology at a private institution of higher education on Long Island, NY. Each student’s record had binary-type information that indicated their grades in mathematics, biology and chemistry classes in their freshman year, as well as their choice of mathematics class; their GPA in the first two semesters; whether they were retained by the school after one year; whether they switched their major; their time and place of graduation, if any, including whether they transferred before graduating; and the number of attempted and completed credits.

The aim of the study was to determine which attributes of a student’s data would be highly relevant to the likelihood of the student graduating; and among graduated students, which attributes were relevant to graduating within 4 years versus in 5 or more years, or to graduating within a STEM field versus changing major to a non-STEM field. Thus, the tests were done targeting a few ‘outcome’ attributes, such as degree major and time to graduation. The article [5] then proposes practical steps based on the findings which can be adopted by universities to potentially improve graduation rates.

The total number of binary attributes in the data is 220, thus, the binary entry table for the D -basis algorithm is of relatively large size 88×220 . Because many of the columns represent a binary encoding of attributes with large ranges of possible results, the density of 1s within the binary table is only 0.14. Tests were only run with target columns 1 through 30, but all columns were present in the input table.

The results of this testing are presented in Appendix A.

For 7 out of the 30 target columns, the target was found to be reducible to (an)other column(s) in the table. In both implementations of the algorithm, this halts execution before hypergraph dualization is called, resulting in nearly identical results between the two versions. On the remaining 23 target columns, however, the Small Space implementation showed significant memory savings over the original version, having an average maximum memory utilization across those 23 columns of only 441 KB compared to the original D -basis’s average of 11.70 MB—a 93.9% average reduction. Across those same 23 target columns, the Small Space implementation saw an increase in the number of processor instructions by an average of 27.2% of the original D -basis’s instruction count, while the average runtime for each column decreased by 23.2% of the original.

4.2 Impostor Phenomenon dataset

Another dataset included in testing involved the standard survey on Impostor Phenomenon (IP), collected for an ongoing analysis project by a collaborator at Queensborough Community College (QCC), Dr. R. Nelson. The impostor phenomenon, or the persistent belief that one’s success results

from luck, mistakes, or others’ misperceptions rather than true ability, has become a key concept for understanding motivation and well-being in higher education [14]. The 20-item Clance Impostor Phenomenon Scale (CIPS) is the most commonly used tool for measuring IP in a person, with score ranges indicating how severe a person’s impostor feelings are. Data collected includes demographic information including age, gender, race/ethnicity, office hours attendance, and tutoring center attendance, as well as a 20-question survey from Clance which yields Likert Scale responses (1-5).

The data set collected by R. Nelson included the survey answers of 84 students in Biology classes at QCC. The initial analysis of these responses are reported in [23]. Another project is currently underway [1] which involves analysis of the implications generated by the D -basis, in addition to the ranking of attributes with respect to particular targets in the dataset. For that project, the data was converted into a binary format, where each question in the 20-item survey was given three binary columns: one for responses at level 4-5 (indicating intense feelings of IP expressed for that question), one for responses at level 3 (medium intensity responses), and the third for responses at level 1-2 (low intensity responses). Other attributes of the participants recorded in the binary table included their gender, age and ethnicity, as well as their participation in office hours and/or tutoring. The goal of the study was to connect these non-survey attributes with higher or lower manifestation of IP in an individuals, given that almost no IP study had ever been conducted on the population of community colleges.

The total input table has the size 84×85 , making it almost square, in contrast with the data in section 4.1. The density of 1s within the binary table is 0.31. Tests were run using all 84 attributes as targets.

The results of this testing are presented in Appendix B. Of the 82 target columns, only one (column 70) was found to be reducible to (an)other column(s) in the table. On the remaining 81 target columns, the Small Space implementation once again showed significant memory savings, a small increase in average instruction count, and a decrease in average runtime. The average maximum memory utilization across the 81 successful target columns was 278 KB, compared to the original D -basis’s average of 33.72 MB, for an average reduction of 97.7%. The number of processor instructions executed by the Small Space implementation increased by an average of 9.3% from the original, while the runtime per target column increased by an average of 31.6% of the original.

Despite fewer attributes being present in this dataset than the STEM data (see 4.1 above), the memory and runtime savings of the Small Space implementation were even more pronounced, and the instruction count increase less severe. This discrepancy is due to the average number of relevant implications produced by each dataset, which stems from the density of 1s in each dataset’s binary table. With similar row counts and identical minimum support thresholds, the higher density of 1s in the Impostor Phenomenon data likely produced more implications than the STEM data, resulting in a longer processing time and a larger list of implications for the original implementation to store.

Acknowledgements. We are grateful to Oren Segal for his guidance in the testing phase of this project. Hofstra University provided virtual machines for remote testing, as well as the financial support for the authors’ attendance of the AMS 2025 Fall Western Sectional meeting in Denver, Colorado, where the results of this paper were reported.

References

- [1] K. Adaricheva, A. Krishnadas, and R. Nelson. *Beyond Total Scores: Item-Level Insights into Impostor Phenomenon in a Community College STEM Setting*. Manuscript, 2025.
- [2] K. Adaricheva, J.B. Nation, and R. Rand. Ordered direct implicational basis of a finite closure system. *Disc. Appl. Math.* 161 (2013), 707–723.
- [3] K. Adaricheva and JB Nation. Discovery of the D -basis in binary tables based on hypergraph dualization. *Theor. Comp. Sci., Part B* 658 (2017), 307–315.
- [4] K. Adaricheva, L. Nourine, and S. Vilmin. Computing the D -base and D -relation in finite closure systems. *Theoretical Computer Science* 1052 (2025), 115459. ISSN: 0304-3975. DOI: 10.1016/j.tcs.2025.115459.

- [5] K. Adaricheva et al. A novel association and ranking approach identifies factors affecting educational outcomes of STEM majors (2025). URL: <https://arxiv.org/pdf/2503.12321>.
- [6] K. Adaricheva et al. Importance of overnight parameters to predict Sea Breeze on Long Island (2023). URL: <https://arxiv.org/pdf/2309.01803>.
- [7] K. Adaricheva et al. Measuring the Implications of the D -basis in Analysis of Data in Biomedical Studies. *Proceedings of ICFCA-15, Nerja, Spain*. Springer, 2015, 39–57.
- [8] M. Babin and S. Kuznetsov. Recognizing Pseudo-intents is coNP-complete. Vol. 672. Jan. 2010, 294–301.
- [9] J.L. Balcázar. Redundancy, deduction schemes, and minimum-size bases for association rules. *Log. Meth. Comput. Sci.* 6 (2010), 1–33.
- [10] M. Barbut and B. Monjardet. *Ordres et classifications: Algèbre et combinatoire*. Paris: Hachette, 1970.
- [11] K. Bertet and B. Monjardet. The multiple facets of the canonical direct unit implicational basis. *Theoretical Computer Science* 411.22-24 (2010), 2155–2166. DOI: 10.1016/j.tcs.2009.12.021.
- [12] K. Bertet et al. Lattices, closures systems and implication bases: A survey of structural aspects and algorithms. *Theoretical Computer Science* 743 (Nov. 2016). DOI: 10.1016/j.tcs.2016.11.021.
- [13] G. Birkhoff. *Lattice theory*. Providence, RI: AMS Colloquium Publications, 1940.
- [14] P. R. Clance and S. A. Imes. The imposter phenomenon in high achieving women: Dynamics and therapeutic intervention. *Psychotherapy: Theory, Research and Practice* (1978). DOI: 10.1037/h0086006.
- [15] K. Elbassioni. On Dualization over Distributive Lattices. *Discrete Mathematics & Theoretical Computer Science* 24.2 (2022): *Discrete Algorithms*. ISSN: 1365-8050. DOI: 10.46298/dmtcs.6742.
- [16] M. Fredman and L. Khachiyan. On the Complexity of Dualization of Monotone Disjunctive Normal Forms. *Journal of Algorithms* 21 (1996), 618–628.
- [17] R. Freese, J. Ježek, and J. B. Nation. *Free Lattices*. Vol. 42. American Mathematical Soc., 1995.
- [18] B. Ganter and R. Wille. *Formal concept Analysis: Mathematical Foundations*. Springer, 1999.
- [19] J.-L. Guigues and V. Duquenne. Familles Minimales d’implications Informatives Résultant d’un Tableau de Données Binaires. *Mathématiques et Sciences humaines* 95 (1986), 5–18.
- [20] M. Kryszkiewicz. Concise Representations of Association Rules. *Proceedings of the ESF Exploratory Workshop on Pattern Detection and Discovery*. Berlin, Heidelberg: Springer-Verlag, 2002, 92–109. ISBN: 3540441484.
- [21] K. Murakami and T. Uno. Efficient algorithms for dualizing large-scale hypergraphs. *Discrete Applied Mathematics* 170 (2014), 83–94.
- [22] JB Nation et al. Combining algorithms to find signatures that predict risk in early-stage stomach cancer. *Journal of Computational Biology* 28 (2021), 985–1006.
- [23] R. K. Nelson and V. A. Muse. Evaluating the Prevalence of Imposter Syndrome Among Community College General Biology Students. *Community College Journal of Research and Practice* (2025), 1–15. DOI: 10.1080/10668926.2025.2476496.
- [24] O. Segal et al. The D -basis algorithm for association rules of high confidence. *IT in Industry* 6 (N3) (2018).
- [25] M. Wild. A theory of finite closure spaces based on implications. *Advances in Mathematics* 108.1 (1994), 118–139.
- [26] M. Wild. The joy of implications, aka pure Horn formulas: mainly a survey. *Theoretical Computer Science* 658 (2017), 264–292. DOI: 10.1016/j.tcs.2016.03.018.

Appendix A STEM dataset test results

This section presents testing results from the STEM dataset. The first column of each table represents the attribute number which served as the target for that test; column numbers marked with a star (*) indicate that the column was reduced to another, and the full algorithm was not executed on that target column. The column ‘Original’ represents the measurement for the existing D -basis implementation. The ‘Small Space’ column represents the same measurement for the Small Space implementation. The ‘Difference’ calculates the change between the ‘Original’ and ‘Small Space’ columns, arranged as ‘Small Space’–‘Original’. Finally, ‘Savings’ represents how much the Small Space result was reduced compared to the original result, calculated as $(\text{‘Original’} - \text{‘Small Space’}) / \text{‘Original’}$ as a percentage.

Table 2: Maximum memory usage (in bytes) for the STEM dataset.

Col #	Original	Small Space	Difference	Savings (%)
1	2,661,392	423,016	-2,238,376	84.11%
2*	251,368	251,368	0	0.00%
3	5,451,088	427,120	-5,023,968	92.16%
4	9,172,992	440,784	-8,732,208	95.19%
5	22,472,784	458,720	-22,014,064	97.96%
6	9,269,984	437,248	-8,832,736	95.28%
7	4,994,224	427,312	-4,566,912	91.44%
8	25,036,160	464,064	-24,572,096	98.15%
9	1,940,624	420,808	-1,519,816	78.32%
10	18,839,376	458,720	-18,380,656	97.57%
11*	248,512	248,512	0	0.00%
12	5,451,088	427,120	-5,023,968	92.16%
13	17,218,544	458,672	-16,759,872	97.34%
14	9,672,928	436,192	-9,236,736	95.49%
15*	248,512	248,512	0	0.00%
16*	248,512	248,512	0	0.00%
17*	248,512	248,512	0	0.00%
18	9,174,048	440,784	-8,733,264	95.20%
19	5,451,344	427,120	-5,024,224	92.16%
20*	248,512	248,512	0	0.00%
21	15,887,904	457,144	-15,430,760	97.12%
22	24,841,312	469,560	-24,371,752	98.11%
23	13,475,312	448,384	-13,026,928	96.67%
24*	248,512	248,512	0	0.00%
25	5,451,088	427,120	-5,023,968	92.16%
26	23,296,784	459,664	-22,837,120	98.03%
27	22,925,024	462,304	-22,462,720	97.98%
28	5,451,088	427,120	-5,023,968	92.16%
29	5,451,088	427,120	-5,023,968	92.16%
30	5,451,088	427,120	-5,023,968	92.16%
AVG	9,025,990	396,522	-8,629,468	71.97%
AVG (no *)	11,697,272	441,444	-11,255,828	93.87%

Table 3: Processor instruction count for the STEM dataset.

Col #	Original	Small Space	Difference	Savings (%)
1	259,219,662	285,606,047	26,386,385	-10.18%
2*	21,470,455	21,472,746	2,291	-0.01%
3	446,731,204	535,105,930	88,374,726	-19.78%
4	624,431,916	844,174,865	219,742,949	-35.19%
5	1,540,918,495	2,117,799,406	576,880,911	-37.44%
6	740,134,187	888,293,413	148,159,226	-20.02%
7	422,419,070	492,330,936	69,911,866	-16.55%
8	1,676,108,597	2,336,879,023	660,770,426	-39.42%
9	213,432,739	223,866,023	10,433,284	-4.89%
10	1,291,678,033	1,770,568,059	478,890,026	-37.08%
11*	21,358,187	21,360,495	2,308	-0.01%
12	443,826,972	530,038,379	86,211,407	-19.42%
13	1,131,936,207	1,553,253,477	421,317,270	-37.22%
14	770,360,286	931,148,031	160,787,745	-20.87%
15*	21,356,440	21,358,789	2,349	-0.01%
16*	21,352,109	21,354,442	2,333	-0.01%
17*	21,366,104	21,368,402	2,298	-0.01%
18	631,424,853	840,320,469	208,895,616	-33.08%
19	442,569,750	540,587,267	98,017,517	-22.15%
20*	21,356,265	21,358,492	2,227	-0.01%
21	1,070,001,335	1,440,965,442	370,964,107	-34.67%
22	1,655,786,304	2,320,861,699	665,075,395	-40.17%
23	918,243,657	1,236,077,111	317,833,454	-34.61%
24*	21,370,155	21,372,479	2,324	-0.01%
25	447,268,388	536,808,081	89,539,693	-20.02%
26	1,514,548,225	2,118,754,978	604,206,753	-39.89%
27	1,506,427,507	2,119,466,728	613,039,221	-40.69%
28	441,493,614	532,217,674	90,724,060	-20.55%
29	444,033,676	534,248,592	90,214,916	-20.32%
30	449,021,118	546,134,346	97,113,228	-21.63%
AVG	641,054,850	847,505,061	206,450,210	-20.86%
AVG (no *)	829,652,861	1,098,935,042	269,282,182	-27.21%

Table 4: Runtime (in milliseconds) for the STEM dataset.

Col #	Original	Small Space	Difference	Savings (%)
1	2,314	1,796	-518	22.39%
2*	433	429	-4	0.92%
3	3,209	2,614	-595	18.54%
4	4,208	3,215	-993	23.60%
5	8,637	6,716	-1,921	22.24%
6	4,706	3,470	-1,236	26.26%
7	3,158	2,405	-753	23.84%
8	9,304	7,274	-2,030	21.82%
9	2,062	1,605	-457	22.16%
10	7,792	6,067	-1,725	22.14%
11*	443	438	-5	1.13%
12	3,237	2,607	-630	19.46%
13	6,918	5,408	-1,510	21.83%
14	5,068	3,736	-1,332	26.28%
15*	440	437	-3	0.68%
16*	440	441	1	-0.23%
17*	438	437	-1	0.23%
18	4,251	3,305	-946	22.25%
19	3,249	2,548	-701	21.58%
20*	438	443	5	-1.14%
21	6,688	5,040	-1,648	24.64%
22	9,768	7,522	-2,246	22.99%
23	5,875	4,410	-1,465	24.94%
24*	439	438	-1	0.23%
25	3,206	2,544	-662	20.65%
26	9,377	6,788	-2,589	27.61%
27	9,211	6,855	-2,356	25.58%
28	3,412	2,521	-891	26.11%
29	3,331	2,631	-700	21.01%
30	3,442	2,543	-899	26.12%
AVG	4,183	3,223	-960	17.86%
AVG (no *)	5,323	4,070	-1,252	23.22%

Appendix B Impostor Phenomenon dataset test results

This section presents testing results from the Impostor Phenomenon dataset. Tables are split across two pages. The first column of each table represents the attribute number which served as the target for that test; column numbers marked with a star (*) indicate that the column was reduced to another, and the full algorithm was not executed on that target column. The column ‘Original’ represents the measurement for the existing D -basis implementation. The ‘Small Space’ column represents the same measurement for the Small Space implementation. The ‘Difference’ calculates the change between the ‘Original’ and ‘Small Space’ columns, arranged as ‘Small Space’–‘Original’. Finally, ‘Savings’ represents how much the Small Space result was reduced compared to the original result, calculated as (‘Original’–‘Small Space’)/‘Original’ as a percentage.

Table 5: Maximum memory usage (in bytes) for the Impostor Phenomenon dataset.

Col #	Original	Reworked	Difference	Savings (%)
1	46,851,344	286,472	-46,564,872	99.39%
2	32,341,808	274,976	-32,066,832	99.15%
3	20,550,752	275,856	-20,274,896	98.66%
4	38,151,696	283,176	-37,868,520	99.26%
5	29,028,080	272,808	-28,755,272	99.06%
6	31,018,816	274,520	-30,744,296	99.11%
7	29,787,824	278,680	-29,509,144	99.06%
8	35,958,048	278,184	-35,679,864	99.23%
9	31,496,336	274,056	-31,222,280	99.13%
10	43,421,696	277,240	-43,144,456	99.36%
11	36,628,944	289,400	-36,339,544	99.21%
12	17,849,360	269,824	-17,579,536	98.49%
13	17,936,032	274,056	-17,661,976	98.47%
14	40,827,760	286,776	-40,540,984	99.30%
15	39,668,096	287,896	-39,380,200	99.27%
16	35,334,352	287,248	-35,047,104	99.19%
17	29,824,144	281,488	-29,542,656	99.06%
18	29,094,880	273,712	-28,821,168	99.06%
19	59,221,744	285,096	-58,936,648	99.52%
20	36,707,872	278,168	-36,429,704	99.24%
21	7,793,872	268,376	-7,525,496	96.56%
22	25,223,472	283,888	-24,939,584	98.87%
23	36,749,328	280,704	-36,468,624	99.24%
24	37,624,784	277,736	-37,347,048	99.26%
25	11,118,784	261,376	-10,857,408	97.65%
26	45,093,936	286,392	-44,807,544	99.36%
27	43,629,536	292,784	-43,336,752	99.33%
28	34,277,456	279,984	-33,997,472	99.18%
29	32,565,920	283,584	-32,282,336	99.13%
30	29,342,032	277,392	-29,064,640	99.05%
31	24,433,456	271,936	-24,161,520	98.89%
32	31,783,264	276,736	-31,506,528	99.13%
33	41,203,584	280,976	-40,922,608	99.32%
34	56,070,896	287,864	-55,783,032	99.49%
35	33,559,312	277,072	-33,282,240	99.17%
36	11,802,512	269,880	-11,532,632	97.71%
37	31,745,232	280,632	-31,464,600	99.12%
38	35,895,104	279,408	-35,615,696	99.22%
39	27,261,568	289,280	-26,972,288	98.94%
40	50,433,536	284,840	-50,148,696	99.44%
41	24,158,944	276,424	-23,882,520	98.86%
42	21,735,024	275,856	-21,459,168	98.73%

Table 6: Maximum memory usage (in bytes) for the Impostor Phenomenon dataset (cont.).

Col #	Original	Reworked	Difference	Savings (%)
43	38,398,640	278,992	-38,119,648	99.27%
44	28,582,928	284,096	-28,298,832	99.01%
45	28,957,264	277,136	-28,680,128	99.04%
46	38,445,136	283,400	-38,161,736	99.26%
47	29,817,392	282,160	-29,535,232	99.05%
48	26,506,528	278,656	-26,227,872	98.95%
49	47,895,456	285,464	-47,609,992	99.40%
50	29,907,264	285,640	-29,621,624	99.04%
51	17,899,648	271,816	-17,627,832	98.48%
52	50,843,456	286,000	-50,557,456	99.44%
53	27,855,968	278,848	-27,577,120	99.00%
54	16,773,216	270,408	-16,502,808	98.39%
55	40,271,808	276,264	-39,995,544	99.31%
56	40,547,184	284,840	-40,262,344	99.30%
57	19,879,776	273,608	-19,606,168	98.62%
58	34,089,376	282,888	-33,806,488	99.17%
59	41,824,032	287,752	-41,536,280	99.31%
60	20,514,176	272,448	-20,241,728	98.67%
61	22,581,088	279,680	-22,301,408	98.76%
62	10,430,336	261,520	-10,168,816	97.49%
63	15,294,080	275,648	-15,018,432	98.20%
64	17,041,104	273,768	-16,767,336	98.39%
65	33,796,480	280,960	-33,515,520	99.17%
66	4,834,176	255,808	-4,578,368	94.71%
67	37,026,528	284,928	-36,741,600	99.23%
68	4,648,352	256,568	-4,391,784	94.48%
69	44,427,680	280,216	-44,147,464	99.37%
70*	153,912	153,912	0	0.00%
71	57,064,064	284,328	-56,779,736	99.50%
72	57,064,512	293,240	-56,771,272	99.49%
73	49,102,688	288,864	-48,813,824	99.41%
74	57,064,064	286,888	-56,777,176	99.50%
75	28,447,824	274,464	-28,173,360	99.04%
76	57,060,384	286,888	-56,773,496	99.50%
77	55,574,688	287,288	-55,287,400	99.48%
78	57,065,120	286,888	-56,778,232	99.50%
79	31,288,800	283,544	-31,005,256	99.09%
80	57,064,160	287,920	-56,776,240	99.50%
81	57,061,024	286,888	-56,774,136	99.50%
82	57,061,840	286,888	-56,774,952	99.50%
AVG	33,723,943	278,174	-33,445,769	97.72%
AVG (no *)	34,138,387	279,708	-33,858,679	98.93%

Table 7: Processor instruction count for the Impostor Phenomenon dataset.

Col #	Original	Reworked	Difference	Savings (%)
1	3,376,218,207	3,897,727,186	521,508,979	-15.45%
2	2,345,920,778	2,543,488,313	197,567,535	-8.42%
3	1,702,812,219	1,732,175,857	29,363,638	-1.72%
4	2,780,812,957	3,123,661,706	342,848,749	-12.33%
5	2,262,360,099	2,356,515,863	94,155,764	-4.16%
6	2,316,620,430	2,551,142,137	234,521,707	-10.12%
7	2,192,583,070	2,427,633,318	235,050,248	-10.72%
8	2,692,793,381	2,992,993,428	300,200,047	-11.15%
9	2,384,711,428	2,530,028,332	145,316,904	-6.09%
10	3,009,707,871	3,537,639,750	527,931,879	-17.54%
11	2,674,852,925	3,022,815,102	347,962,177	-13.01%
12	1,485,488,714	1,452,462,104	-33,026,610	2.22%
13	1,452,080,282	1,416,728,441	-35,351,841	2.43%
14	2,944,386,203	3,349,949,274	405,563,071	-13.77%
15	2,893,228,669	3,295,851,559	402,622,890	-13.92%
16	2,458,704,860	2,833,800,244	375,095,384	-15.26%
17	2,316,520,892	2,459,936,172	143,415,280	-6.19%
18	2,150,297,250	2,379,146,312	228,849,062	-10.64%
19	4,022,275,552	4,970,319,407	948,043,855	-23.57%
20	2,679,759,418	2,974,571,023	294,811,605	-11.00%
21	703,463,805	638,131,111	-65,332,694	9.29%
22	1,964,764,830	2,022,186,915	57,422,085	-2.92%
23	2,738,307,695	2,986,911,992	248,604,297	-9.08%
24	2,790,374,978	3,149,212,717	358,837,739	-12.86%
25	911,785,305	850,605,320	-61,179,985	6.71%
26	3,211,760,803	3,803,336,271	591,575,468	-18.42%
27	3,168,335,362	3,615,653,420	447,318,058	-14.12%
28	2,419,412,809	2,745,922,866	326,510,057	-13.50%
29	2,420,277,009	2,648,438,942	228,161,933	-9.43%
30	2,260,445,404	2,391,326,945	130,881,541	-5.79%
31	1,816,664,367	1,918,138,119	101,473,752	-5.59%
32	2,397,763,189	2,666,774,181	269,010,992	-11.22%
33	2,991,123,084	3,377,913,245	386,790,161	-12.93%
34	3,844,679,590	4,725,941,968	881,262,378	-22.92%
35	2,474,068,950	2,764,113,691	290,044,741	-11.72%
36	1,031,391,498	954,087,345	-77,304,153	7.50%
37	2,275,096,403	2,563,503,007	288,406,604	-12.68%
38	2,670,773,992	3,011,679,971	340,905,979	-12.76%
39	2,032,363,292	2,204,499,813	172,136,521	-8.47%
40	3,470,198,262	4,136,390,466	666,192,204	-19.20%
41	1,836,945,344	1,942,781,507	105,836,163	-5.76%
42	1,751,939,066	1,810,911,823	58,972,757	-3.37%

Table 8: Processor instruction count for the Impostor Phenomenon dataset (cont.).

Col #	Original	Reworked	Difference	Savings (%)
43	2,672,641,534	3,077,886,130	405,244,596	-15.16%
44	2,126,503,688	2,316,126,293	189,622,605	-8.92%
45	2,294,398,823	2,413,878,797	119,479,974	-5.21%
46	2,707,923,568	3,073,542,252	365,618,684	-13.50%
47	2,255,694,710	2,423,132,828	167,438,118	-7.42%
48	2,010,807,264	2,186,737,000	175,929,736	-8.75%
49	3,211,864,565	3,860,903,804	649,039,239	-20.21%
50	2,195,987,533	2,386,007,519	190,019,986	-8.65%
51	1,484,473,780	1,510,463,131	25,989,351	-1.75%
52	3,474,453,036	4,170,517,712	696,064,676	-20.03%
53	2,052,465,393	2,246,912,091	194,446,698	-9.47%
54	1,374,830,920	1,396,419,676	21,588,756	-1.57%
55	2,823,154,336	3,238,543,318	415,388,982	-14.71%
56	2,871,834,399	3,335,996,148	464,161,749	-16.16%
57	1,711,032,602	1,646,855,305	-64,177,297	3.75%
58	2,461,425,678	2,786,321,032	324,895,354	-13.20%
59	3,034,523,312	3,524,744,895	490,221,583	-16.15%
60	1,670,468,014	1,645,540,876	-24,927,138	1.49%
61	1,786,847,550	1,835,409,722	48,562,172	-2.72%
62	966,102,306	842,132,346	-123,969,960	12.83%
63	1,362,956,510	1,284,451,702	-78,504,808	5.76%
64	1,348,393,886	1,314,296,172	-34,097,714	2.53%
65	2,549,333,312	2,860,461,027	311,127,715	-12.20%
66	475,778,484	388,879,974	-86,898,510	18.26%
67	2,741,164,921	3,100,413,453	359,248,532	-13.11%
68	491,867,246	375,267,467	-116,599,779	23.71%
69	3,214,910,473	3,590,034,969	375,124,496	-11.67%
70*	11,342,090	11,344,358	2,268	-0.02%
71	4,073,761,683	4,800,874,451	727,112,768	-17.85%
72	4,053,571,331	4,794,933,343	741,362,012	-18.29%
73	3,590,405,517	4,187,520,444	597,114,927	-16.63%
74	4,026,625,955	4,787,655,260	761,029,305	-18.90%
75	2,148,372,095	2,319,198,209	170,826,114	-7.95%
76	4,053,990,254	4,810,874,225	756,883,971	-18.67%
77	3,865,721,748	4,657,316,297	791,594,549	-20.48%
78	4,054,340,787	4,840,687,647	786,346,860	-19.40%
79	2,147,745,069	2,509,059,770	361,314,701	-16.82%
80	4,031,960,442	4,798,538,951	766,578,509	-19.01%
81	4,042,096,459	4,843,629,108	801,532,649	-19.83%
82	4,043,386,094	4,801,177,008	757,790,914	-18.74%
AVG	2,473,649,117	2,777,704,047	304,054,930	-9.20%
AVG (no *)	2,504,047,969	2,811,856,636	307,808,667	-9.31%

Table 9: Runtime (in milliseconds) for the Impostor Phenomenon dataset.

Col #	Original	Reworked	Difference	Savings (%)
1	17,959	12,420	-5,539	30.84%
2	13,028	8,370	-4,658	35.75%
3	9,739	6,244	-3,495	35.89%
4	15,397	10,235	-5,162	33.53%
5	12,673	8,000	-4,673	36.87%
6	12,993	8,757	-4,236	32.60%
7	12,088	8,243	-3,845	31.81%
8	14,636	10,116	-4,520	30.88%
9	15,667	8,479	-7,188	45.88%
10	16,559	11,488	-5,071	30.62%
11	14,395	9,961	-4,434	30.80%
12	8,655	5,620	-3,035	35.07%
13	8,357	5,165	-3,192	38.20%
14	15,619	11,404	-4,215	26.99%
15	15,311	11,346	-3,965	25.90%
16	13,047	9,550	-3,497	26.80%
17	12,698	8,503	-4,195	33.04%
18	11,804	8,219	-3,585	30.37%
19	20,434	15,964	-4,470	21.88%
20	14,175	9,900	-4,275	30.16%
21	4,603	2,988	-1,615	35.09%
22	11,266	6,891	-4,375	38.83%
23	14,717	9,885	-4,832	32.83%
24	14,739	10,584	-4,155	28.19%
25	5,767	3,522	-2,245	38.93%
26	16,817	12,458	-4,359	25.92%
27	16,601	12,026	-4,575	27.56%
28	13,100	9,191	-3,909	29.84%
29	13,289	8,810	-4,479	33.70%
30	12,420	8,189	-4,231	34.07%
31	10,193	6,567	-3,626	35.57%
32	13,002	9,100	-3,902	30.01%
33	16,055	11,213	-4,842	30.16%
34	19,774	15,187	-4,587	23.20%
35	13,232	9,278	-3,954	29.88%
36	6,301	3,906	-2,395	38.01%
37	12,356	8,751	-3,605	29.18%
38	14,136	9,954	-4,182	29.58%
39	11,188	7,617	-3,571	31.92%
40	17,727	13,370	-4,357	24.58%
41	10,274	6,771	-3,503	34.10%
42	9,865	6,588	-3,277	33.22%

Table 10: Runtime (in milliseconds) for the Impostor Phenomenon dataset (cont.).

Col #	Original	Reworked	Difference	Savings (%)
43	14,269	10,141	-4,128	28.93%
44	11,761	7,918	-3,843	32.68%
45	12,519	8,270	-4,249	33.94%
46	14,522	10,185	-4,337	29.87%
47	12,320	8,392	-3,928	31.88%
48	11,489	7,577	-3,912	34.05%
49	17,070	12,650	-4,420	25.89%
50	12,004	8,006	-3,998	33.31%
51	8,458	5,651	-2,807	33.19%
52	17,945	13,429	-4,516	25.17%
53	11,450	7,829	-3,621	31.62%
54	8,042	5,216	-2,826	35.14%
55	15,411	10,733	-4,678	30.35%
56	15,156	11,045	-4,111	27.12%
57	9,564	5,894	-3,670	38.37%
58	13,189	9,268	-3,921	29.73%
59	15,973	11,567	-4,406	27.58%
60	9,421	5,859	-3,562	37.81%
61	10,198	6,560	-3,638	35.67%
62	6,072	3,542	-2,530	41.67%
63	8,023	4,976	-3,047	37.98%
64	7,923	4,919	-3,004	37.91%
65	13,687	9,673	-4,014	29.33%
66	3,653	2,215	-1,438	39.36%
67	14,617	10,201	-4,416	30.21%
68	3,703	2,280	-1,423	38.43%
69	17,155	11,664	-5,491	32.01%
70*	451	432	-19	4.21%
71	20,549	15,422	-5,127	24.95%
72	20,693	15,134	-5,559	26.86%
73	18,652	13,433	-5,219	27.98%
74	20,665	15,383	-5,282	25.56%
75	12,214	7,582	-4,632	37.92%
76	20,723	15,090	-5,633	27.18%
77	19,777	14,563	-5,214	26.36%
78	20,575	14,988	-5,587	27.15%
79	11,739	8,319	-3,420	29.13%
80	20,477	14,993	-5,484	26.78%
81	20,501	14,962	-5,539	27.02%
82	20,415	15,146	-5,269	25.81%
AVG	13,362	9,292	-4,070	31.27%
AVG (no *)	13,521	9,401	-4,120	31.61%